LA-UR-23-30913

Approved for public release; distribution is unlimited.

Title:	Beam Optics Studies for Larger Beampipe Diameters for the LAMP-PSR
Author(s):	Yoskowitz, Joshua Tyler Huang, En-Chuan
Intended for:	Report
Issued:	2023-09-25

LANSCE MODERNIZATION PROJECT

Beam Optics Studies for Larger Beampipe Diameters for the LAMP-PSR

J. T. Yoskowitz and E-. C. Huang

Report #: LA-UR-23-?????
September 21, 2023

Los Alamos NATIONAL LABORATORY

NNSA

Table of Contents

Introduction

The proposed beampipe diameter increase of the PSR beamlines for the LAMP PSR upgrade is expected decrease beam loss due to tuning errors and misalignment. However, a larger beampipe diameter would require increasing the pole-to-pole gap height within all magnets in the PSR (dipole gap, quadrupole bore, etc.). This would in turn affect the extent and profile of the fringe fields at the ends of the magnets, altering the effective length of the magnets and thus the magnetic optics. In this work, we used the simulation code MAD-X [1] to model the PSR lattice for different beampipe diameters. The results of these simulations will be later used to benchmark particle simulations using the code pyORBIT. The MAD-X simulations are described, and the simulation results are discussed in this technote.

1 PSR MAD-X Model

Figure 1 shows a schematic of the PSR depicting beamline elements that constitute the PSR's magnetic lattice: dipoles, quadrupoles, kickers, and steerers. The PSR consists of ten sectors, each composed of a FODO lattice between two halves of a dipole. That is, each sector contains the elements (in order): half-dipole, drift, horizontally focusing quadrupole, drift, horizontally defocusing quadrupole, drift, half-dipole. Dipoles SRBM21 thru SRBM91 each bend the beam 36°. In sector 0, used for beam injection and extraction, the dipole SRBM01 bends the beam 32.8° to accommodate the injected beam at the merging magnet RIBM09, which bends the beam 6.8°. Dipoles SRBM11 and SRBM12 each bend the beam 16.2° to compensate for the broken 10-fold symmetry of the PSR. The trajectory of the beam through a given dipole depends on the dipole length, bending angle, beam entrance and exit angles relative to the dipole pole faces, gap height between the poles, and the field strength. Figure 2 shows a diagram of the trajectory of a charged particle through a dipole magnet with bending radius ρ and total bend angle θ. The blue profile represents a "rectangular" bend magnet, where the beam trajectory makes an angle of $\frac{\theta}{2}$ relative to the normal to the dipole pole faces at both the entrance and exit of the dipole. The black outline shows a "sector" bend magnet, where the beam trajectory is normal to the pole faces at both the entrance and exit of the dipole.

Simulations were performed using MAD-X to determine the Twiss parameters along the reference orbit for different dipole gap heights and fringe field integrals. In each simulation, a proton beam with the PSR design energy of 1.733 GeV is tracked through the PSR lattice beginning and ending at the upstream edge of dipole SRBM01 (in sector 9). The PSR lattice file used in the simulations was originally created by J. Kolski in 2011 [2]. The optical parameters of the beam are calculated at each element in the lattice.

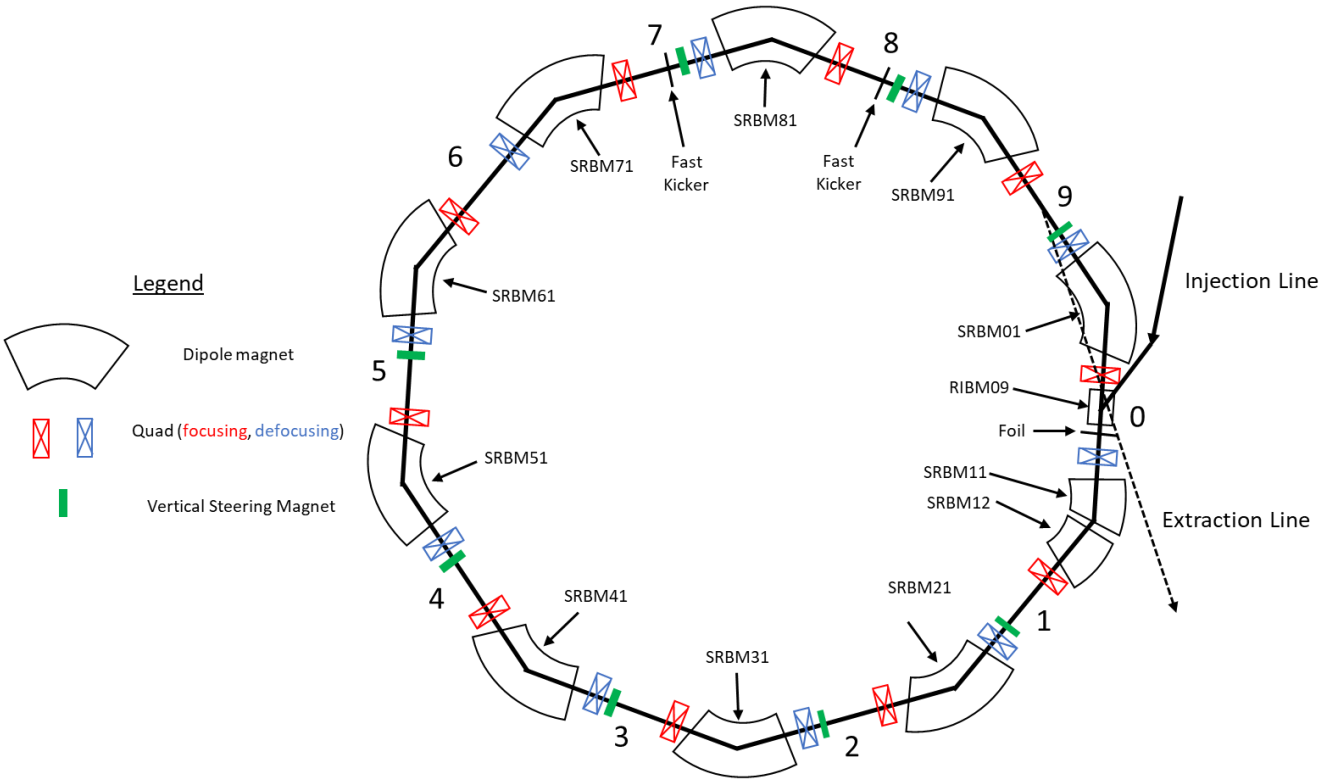

Figure 1: Schematic of the PSR depicting the magnetic beamline elements (dipoles, quadrupoles, steerers), fast kickers, foil, injection and extraction lines, and beamline numbers (0-9).

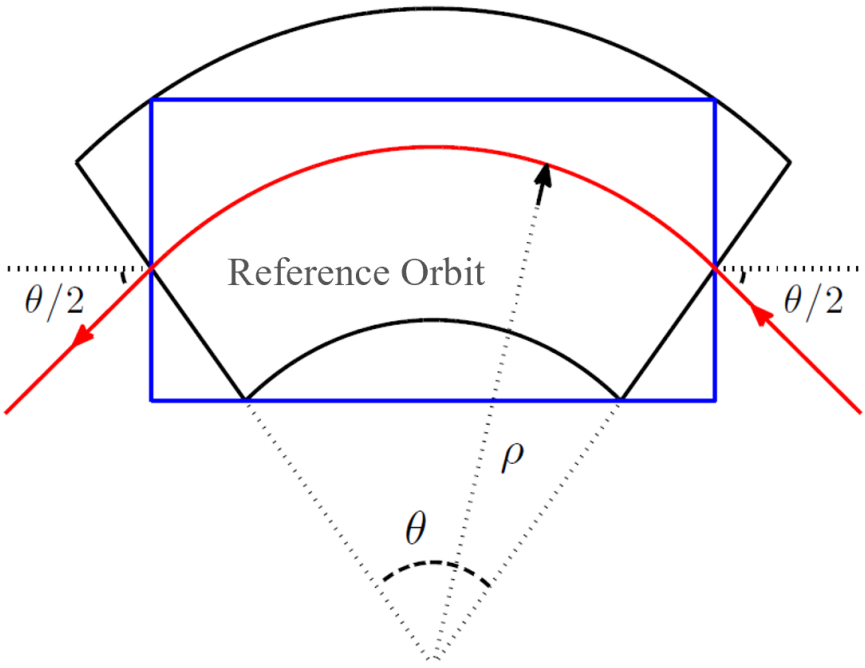

Figure 2: Diagram of the trajectory of a charged particle through a rectangular magnet (blue outline) with bending radius ρ and incident angle $\frac{\theta}{2}$ [3]. The black outline represents a sector magnet with the particle trajectory incident normal to the entrance and exit pole faces.

Of particular interest are the fringe fields at the edges of the dipole magnets. The PSR dipoles are rectangular magnets with the edge angle equal to one half of the bending angle. The transfer matrix for a rectangular magnet in the y-direction (vertical) can be written as [3]:

$$M_y = \begin{pmatrix} 1 - \theta \tan\left(\frac{\theta}{2} - \zeta\right) & \rho\theta \\ \frac{1}{\rho}\tan^2\left(\frac{\theta}{2} - \zeta\right) - \frac{2}{\rho}\tan\left(\frac{\theta}{2} - \zeta\right) & 1 - \theta \tan\left(\frac{\theta}{2} - \zeta\right) \end{pmatrix}$$

where the factor $\zeta = \frac{g\kappa}{\rho}\sec\left(\frac{\theta}{2}\right)\left(1 + \sin^2\left(\frac{\theta}{2}\right)\right)$ is a correction factor to the dipole focal length due to the fringe fields. The factor g is the full gap height, and the factor κ, given by

$$\kappa = \int_{-\infty}^{\infty} \frac{B_y(s)(B_0 - B_y(s))}{g \cdot B_0^2} ds,$$

is the fringe field integral, which characterizes the extent of the fringe fields (i.e., the effective length). In MAD-X, the effects of dipole fringe fields are incorporated by setting the attributes FINT $(= \kappa)$ and HGAP $\left(= \frac{g}{2}\right)$. Common approximations for FINT, which are studied in this work, are listed in Table 1.

Table 1: Values for different approximations of the fringe field integral FINT [1].

Fringe Field Integral Approximation	Value
Hard Edge	0
Linear Field Decay	0.17
Clamped "Rogowski" Fringe Field	0.4
"Square-Edged" Non-Saturating Magnet	0.45
Unclamped "Rogowski" Fringe Field	0.7

The fringe field integral of each PSR dipole was estimated by J. Kolski et al. using the method of ray tracing [3], in which parallel rays were traced through the entrance edge to the exit of a TOSCA 3D simulation model of the dipole to determine its focal length f, given by

$$f = \frac{\rho}{\tan\left(\frac{\theta}{2} - \zeta\right)}$$

Since the focal length depends on ζ, and hence κ, estimates of the dipole focal length via ray tracing can be used to calculate the fringe field integral. Ray tracing results by D. Barlow show vertical focusing of the rays (in the y-direction) upon exiting the dipole [4]. The focal length of each dipole can be calculated by determining where the rays intercept the reference orbit. The focal lengths, bending angles, full gap heights and estimated fringe field integrals are listed in Table 1. The long focal length of RIBM09 is due to its small bending angle.

Table 2: PSR dipole bending angles, nominal edge angles, focal lengths, full gap heights, and fringe field integrals [3].

Dipole	Bending Angle (°)	Nominal Edge Angle (°)	Focal Length (m)	Full Gap Height (in)	Fringe Field Integral
SRBM01	32.8	16.4	13.733	4.1252	1.2908
SRBM21 thru SRBM91	36	18	13.733	4.1252	0.90291
RIBM09	6.8	3.4	238.96	5.0598	0.47085
SRBM11	16.2	8.1	32.389	7.1098	0.46491
SRBM12	16.2	8.1	30.889	5.0598	0.52685

2 MAD-X Simulations

MAD-X simulation studies were performed to study the effect of varying the gap height and the fringe field integral on the beam optical parameters, namely the Twiss parameters $\alpha_{x(y)}$ and $\beta_{x(y)}$, the transverse dispersion functions $D_{x(y)}$, and the betatron phase advance $\mu_{x(y)} = \int \frac{ds}{\beta_{x(y)}}$. To obtain baseline plots of these parameters through the PSR lattice, a simulation was performed using the initial parameters in Table 2. These plots, shown in Figure 3, show the proton beam undergoing a single betatron oscillation per sector for a total of 10 oscillations. Figure 4 shows the change in each optical parameter when the gap height of each dipole is increased from 4" to either 5" or 6" for each fringe field integral approximation in Table 1. While there is an increase in the betatron oscillation amplitude due to fringe fields, this effect is over two orders of magnitude smaller in the horizontal direction than in the vertical direction, so only the relative changes in the vertical plane are shown. In particular, the amplitude of the α, β, and D functions are increased in proportion to the value of FINT and HGAP. Physically, this means that as the extent of the fringe fields is increased by a larger dipole gap height or a stronger dipole field, protons spend a longer time within the fringe field and thus are impacted more by its vertical focusing effect. As the average β function increases, μ decreases, implying that increasing FINT and/or HGAP results in a smaller phase advance around the ring. However, $\Delta\mu \ll \mu$ by almost two orders of magnitude, so the tune shift is likely negligible.

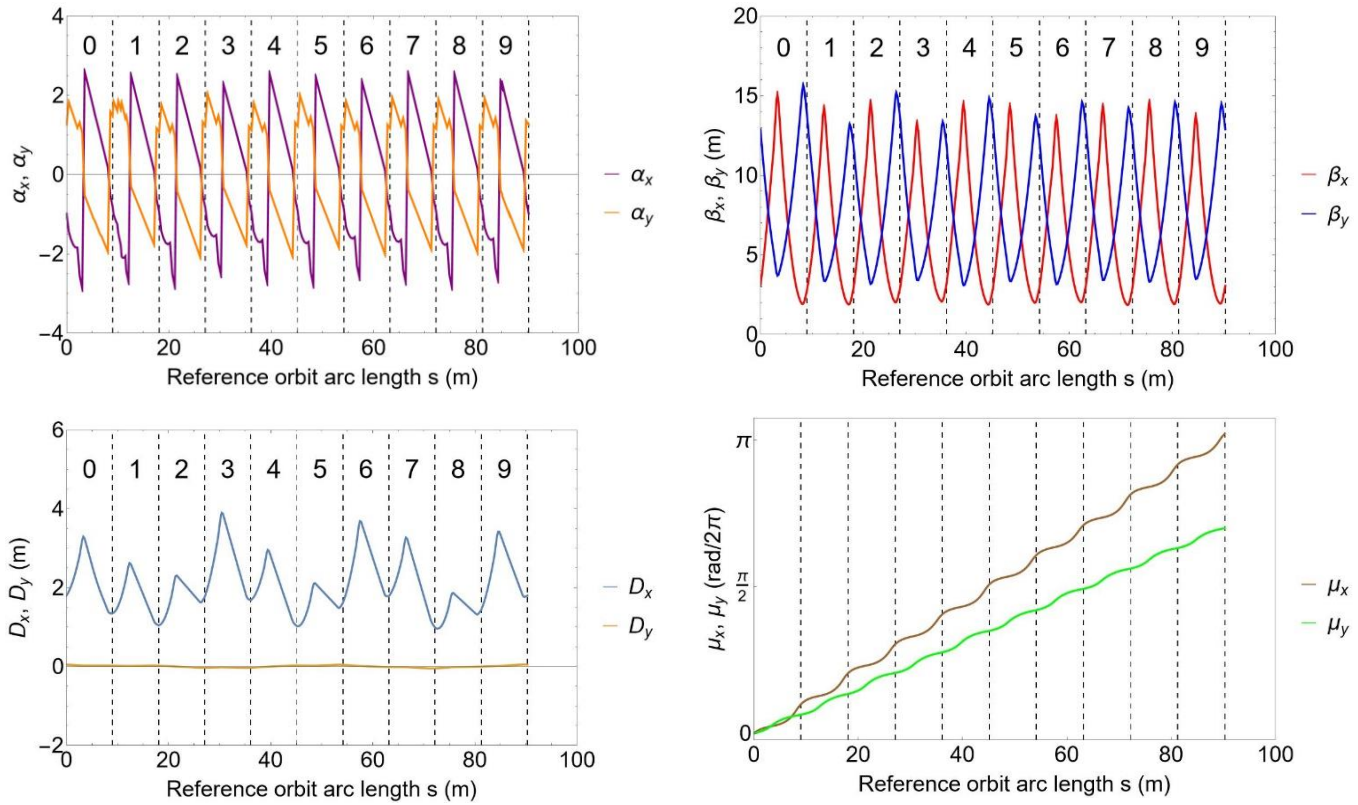

Figure 3: Plots of the beam optical parameters α, β, D, and μ along the PSR lattice in the x- and y-directions. The numbers and dashed lines denote the PSR beamlines 0-9.

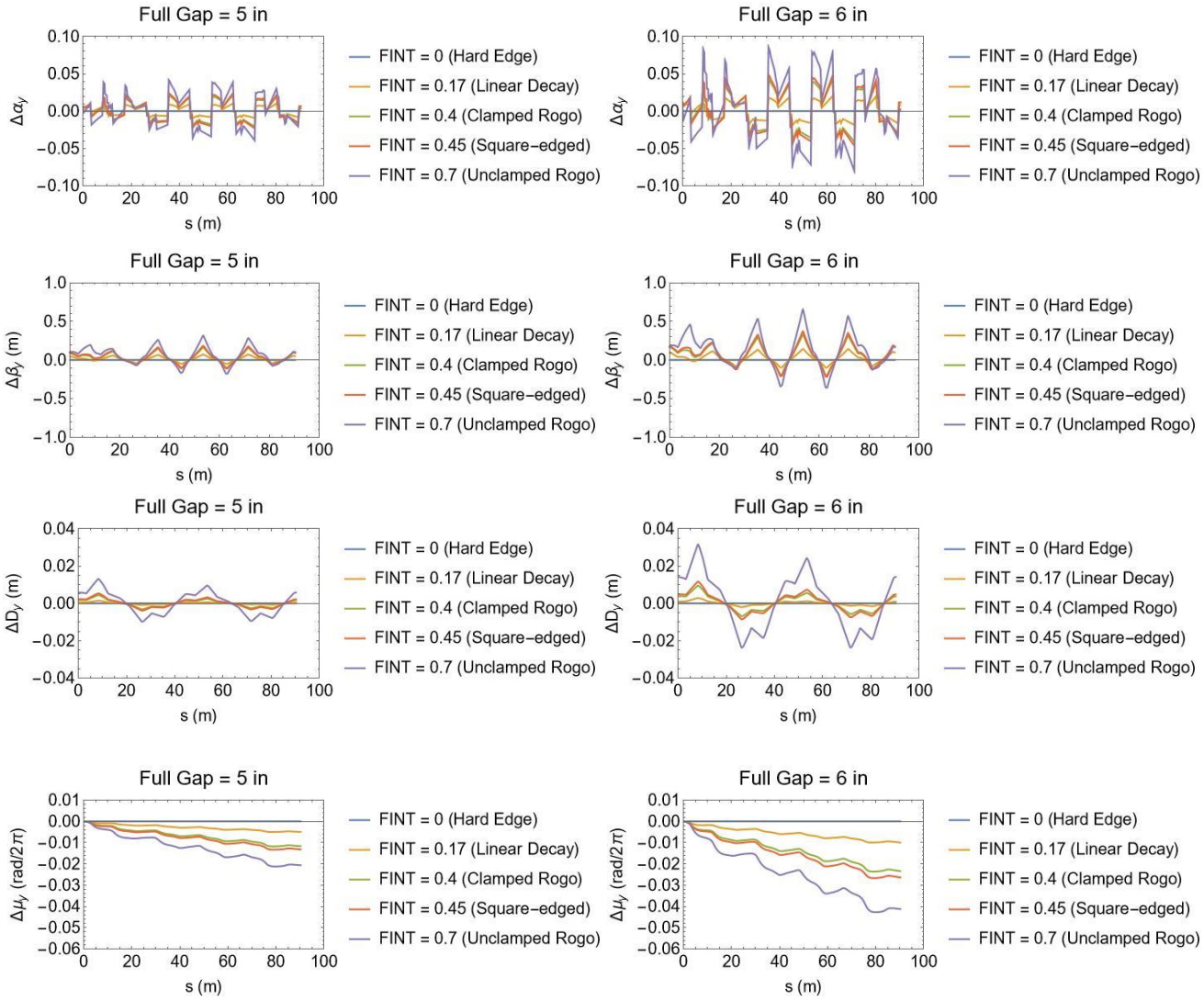

Figure 4: Plots of the relative change of each optical parameter in the transverse direction when the dipole gap height is increased to 5" or 6" from 4" for each FINT approximation.

3 Conclusions and Next Steps

Based on the results of the PSR MAD-X simulations, an increase in gap height or fringe field integral will impact the beam optics, mostly in the vertical plane, but the effect is likely to be negligible. These results will be compared with pyORBIT simulations of the PSR beam dynamics to confirm that an increase in the gap and/or fringe field integral does not significantly impact the beam optics.

Follow-on studies should extend this work in several directions. First, the quadrupole gaps should also be increased to match the dipole gap, and fringe-field effects added to assess the effect on the lattice optics. The resulting lattice model should be used to verify that physically, the required pole-tip fields are feasible.

The PSR's dynamic aperture is an important parameter to consider when attempting to minimize beam losses; the effects of larger magnet gap upon the dynamic aperture needs to be assessed as part of determining whether increasing the

beam pipe is likely to help reduce losses. The impact of magnet field and alignment errors must also be assessed to determine the impact on the dynamic aperture and provide relevant tolerances to the magnet and support system design process.

References

[1] MAD-X code, http://madx.web.cern.ch/madx/.

[2] J. Kolski, "Lattice Modeling and Application of Independent Component Analysis to High Power, Long Bunch Beams in the Los Alamos Proton Storage Ring", Ph.D. thesis, Phys. Dept. Indiana University, Bloomington, IN, 2010.

[3] J. Kolski, D. Barlow, R. Macek, and R. McCrady, "Ray Tracing through the Edge Focusing of Rectangular Benders and an Improved Model for the Los Alamos Proton Storage Ring", LA-UR-11-10334, PSR-11-003.

[4] D. Barlow, "Ring Bender k1.xls".